HHS Public Access

Author manuscript

Cell Rep. Author manuscript; available in PMC 2015 November 21.

Published in final edited form as:

Cell Rep. 2015 November 17; 13(7): 1327–1335. doi:10.1016/j.celrep.2015.10.005.

Slow-γ rhythms coordinate cingulate cortical responses to hippocampal sharp-wave ripples during wakefulness

Miguel Remondes[*] and **Matthew A Wilson**

The Picower Institute for Learning and Memory, Department of Brain and Cognitive Sciences, Massachusetts Institute of Technology, Cambridge, MA 02139, USA

Abstract

Behavioral changes in response to reward require monitoring past behavior relative to present outcomes. This is thought to involve a fine coordination between the hippocampus, which stores and replays memories of past events, and cortical regions such as cingulate cortex, responsible for behavioral planning. Sharp-wave ripple (SWR)-mediated memory replay in the hippocampus of awake rodents contributes to learning, but cortical responses to hippocampal SWR during wakefulness are not known. We now show that in rats, during quiet-wakefulness, cingulate neurons exhibit significant responses to SWR, as well as increased modulation by the accompanying hippocampal LFP slow-γ oscillation, a rhythm associated with intra-hippocampal information processing. The magnitude of cingulate neurons' responses to SWR is significantly correlated with the degree of their modulation by HIPP slow-γ. We hypothesize that, during pauses, cingulate neurons transiently access episodic information concerning previous choices, replayed by HIPP SWR, to evaluate past trajectories in light of their outcome.

Graphical abstract

Correspondence mremondes@medicina.ulisboa.pt.

[*]Present address: Instituto de Medicina Molecular, Faculdade de Medicina da Universidade de Lisboa, Lisbon, 1649-028, Portugal

Author contributions: M.R. conducted the experiments, M.R. and M.W.L. designed the experiments, analyzed the data, and wrote the paper.

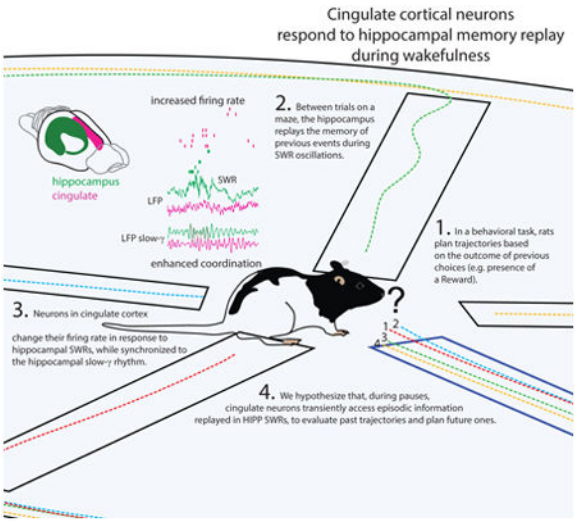

Keywords

Quiet wakefulness; hippocampal sharp-wave ripples; cortical responses; cingulate cortex; slow-γ synchrony

Introduction

Coordinated activity between the hippocampus (HIPP) and neocortex is hypothesized to underlie the progressive extraction of contextual rules, to inform future choices (Foster and Wilson, 2006; Squire et al., 1984). If this is correct, then the anatomical connections known to exist between structures of the Papez circuit, including the hippocampal formation (HIPP), mammillary bodies, thalamus, and cortex, shall preferentially channel this information (Battaglia et al., 2011; Belluscio et al., 2012; Buzsaki, 1989; Jones and Wilson, 2005; Remondes and Schuman, 2002; Siapas et al., 2005). Recent findings show that HIPP high-amplitude/high-frequency neural depolarization events (sharp-wave ripples – SWR) support learning (Ego-Stengel and Wilson, 2010; Girardeau et al., 2009; Jadhav et al., 2012), possibly through the reenactment of neural sequences corresponding to recent episodes (Davidson et al., 2009; Foster and Wilson, 2006; Pezzulo et al., 2014). Synchronous activity between the cortex and HIPP during these events would allow the evaluation of previous choices relative to a present reinforcement, by cortical areas such as cingulate cortex (CG), whose neurons are connected to the hippocampal formation both anatomically (Cenquizca and Swanson, 2007; Jones and Witter, 2007), and functionally (Remondes and Wilson, 2013; Young and McNaughton, 2009a).

The CG exhibits dynamic coordination with HIPP at theta frequency, during random foraging (Young and McNaughton, 2009), as well as during trials of a reinforcement-guided spatial sequential behavior, the Wagon Wheel Maze task, coinciding with increased processing of choice-relevant information (Remondes and Wilson, 2013). It is possible that, between consecutive trials, cingulate cortex evaluates past episodes replayed in HIPP during SWR, to plan the upcoming choice and control subsequent behavior accordingly. In such a

scenario, CG should consistently change its activity during hippocampal SWR, when the rat is motionless and alert between trials on the behavioral apparatus. To test this, we recorded single neuron spikes and local field potential (LFP) from both CG and HIPP, while animals paused between trials of the Wagon Wheel Maze task, in which rats choose sequentially from four distinct trajectories, as previously published (Remondes and Wilson, 2013).

Results

Cingulate neurons change their firing rate during hippocampal SWR events in alert wakefulness

We found that while rats are motionless but alert on the behavior apparatus, HIPP exhibits SWR events, during which subsets of both HIPP and CG neurons increase their firing rate (Figure 1A). In order to test whether, and how many, CG or HIPP neurons significantly change their firing during hippocampal SWR, we extracted +/- 0.5 sec epochs triggered to time points in which: the rat was immobile and alert on the WWM, and the band-pass (150-250 Hz) filtered LFP, as well as hippocampal multi-unit activity, crossed a threshold of 3 SD above the mean (please see Methods, Figure 1A and Figure S1). We subsequently confirmed visually the presence of SWR. During periods of quiet wakefulness SWR, 40/224 (18%) CG neurons significantly change their firing rate (Figure 1B, left column plots, $p<0.05$, Kruskal-Wallis). As previously described (Zhang et al., 1998), the majority (75%) of HIPP neurons also significantly increase their firing rate (Figure 1B, right column plots).

Our SWR detection algorithm captures the point where a SWR is manifested by a 3SD increase in the LFP ripple power and MUA spiking rate, but fails to detect the moment when neural activity from both brain areas changes relative to a pre-SWR baseline - the beginning of the SWR event - which falls below the 3SD cutoff necessary for the algorithm to be specific. To determine this point we averaged all spikes from CG and from HIPP regions across all SWR events (~2962), binned at 5ms, as well as the CG and HIPP LFP during these periods. We found a 80ms gap between the time at which, on average, both the HIPP LFP and MUA exhibit a significant change ($p<0.000001$, Kruskal-Wallis followed by multiple comparisons), here called the SWR “start” (Figure 1C red vertical line), and the time at which a SWR event is detected by our algorithm (Figure 1C, grey vertical line). Similar analysis performed at the same time points, but on CG data, shows that a significant increase in MUA and LFP activity in this region accompanies the changes seen in HIPP, but 75ms and 86ms later, respectively (Figure 1C, right column). This delay is in line with our previous findings for HIPP-CG time offset during behavioral periods dominated by theta (Remondes and Wilson, 2013), suggesting that equivalent circuitry is now active during HIPP SWR. These results indicate that a contingent of CG neurons significantly depolarizes, and increases its firing rate, during quiet wakefulness SWR, instances shown by previous work to elicit the HIPP replay of past experience, and to be critical for learning (Davidson et al., 2009; Jadhav et al., 2012).

In order to understand the nature of SWR-mediated CG-HIPP communication, as well as its significance for information processing, we decided to explore its physiological underpinnings.

Slow γ-rhythms coordinate cingulate and hippocampal LFP during SWR

Oscillatory activity is one of the main neurophysiological correlates of contextual information processing (Wilson et al., 2015). Gamma oscillations have been implicated in the high-level processing of sensory information, in the service of diverse cognitive functions, by coordinating in time the neural activity from distant brain regions (Gray and Singer, 1989; Spellman et al, 2015). Recent studies show that slow-γ oscillations synchronize the activity of hippocampal neurons from distinct sub-fields CA1 and CA3, while SWR events in wakefulness replay past episodes (Carr et al, 2012), precisely the behavior epochs we now focus on. So alongside the raw LFP corresponding to SWR events, we plotted the γ-filtered CG and HIPP LFP, and noticed the presence of transient slow-γ oscillations surrounding SWR (Figures 1A and 3A). We therefore hypothesized that oscillations within this frequency range might also serve to synchronize CG with HIPP, through above-mentioned anatomical connections between these two structures (Cenquizca and Swanson, 2007; Jones and Witter, 2007). To test this hypothesis we computed, for overlapping 250ms windows during SWR epochs, the coherence between CG and HIPP LFP (Figure 2, see Methods). During HIPP SWR, CG and HIPP power, as well as CG-HIPP coherence, were augmented over a range of frequencies, notably γ (Figure 2A, example from one dataset). To determine which of these rhythms is coupled between CG and HIPP, in a manner that is time-locked to HIPP SWR, for each frequency we compared the coherence corresponding to non-overlapping 250ms time bins surrounding (+/- 500ms) the SWR detection trigger, corrected for a baseline (coherence in the 250ms just before the SWR detection). We found that CG-HIPP coherence exhibits an increase, after SWR, in the slow-γ range (26-29 Hz, shown is the plot for 27Hz) (Figure 2B, left panel, *, p=0.006, Kruskal-Wallis followed by multiple comparisons). LFP is susceptible to volume conduction and to motion-related changes. In order to confirm that we are looking at a phenomenon not dependent on such changes, we performed the exact same analysis described above, only using the unsmoothed 5ms binned multi-unit spiking activity (MUA) from hippocampal and cingulate populations. The results of such analyses confirm the presence of a SWR-triggered increase in slow-γ coupling between multi-unit spikes in CG and HIPP (Figure 2B, right panel, *, p=0.03, Kruskal-Wallis followed by multiple comparisons).

A significant increase in CG MUA in response to HIPP SWR happens somewhat earlier than in CG LFP (11ms earlier, see above and Figure 1C). In addition, MUA shows considerable CG-HIPP slow-γ coupling before the baseline considered for the present analysis. These findings, irrespective and in addition to a SWR-triggered increase, suggest that the dynamic of CG-HIPP coordination surrounding SWR events is richer than so far we show. To analyze the dynamic of slow-γ coupling in increased temporal detail, we plotted the slow-γ CG-HIPP coherence of both LFP and MUA, on every 10ms-sliding 250ms windows (Figure 2C). This analysis showed that the slow-γ coupling seen before the baseline considered for the SWR-triggered analysis, exhibits its own dynamic, seemingly specific to each of the two types of neural activity considered, LFP and MUA. While the LFP coherence gradually increases from the baseline point to the SWR detection point, MUA coherence exhibits a distinct peak before the SWR starting point, and considerable coherence levels before the baseline point. Thus, the above data and considerations indicate that a dynamic slow-γ co-modulation of CG and HIPP spikes precedes the occurrence of

HIPP SWR. This is in line with our CG-HIPP slow-γ phase offset findings and with our CG single-unit analyses (as we'll present below), in that the engagement of CG neurons to HIPP slow-γ increases during quiet wakefulness before the occurrence of SWR (Figure 4B). Furthermore, the fact that a SWR-related increase in spike coherence precedes a corresponding increase in LFP coherence suggests that the synchronicity of neuronal spikes precedes the synchronicity of somato-dendritic processing, and that an initial message carried by slow-γ-modulated spikes, is followed by synchronized dendritic processing of the contents thereof.

Hippocampus and Cingulate LFP are slow-γ phase-locked during HIPP SWR

A closer look at the raw and γ-filtered CG and HIPP LFP during SWR epochs reveals not only the presence of sustained slow-γ oscillations, but also epochs characterized by peak-to-peak temporal alignment between filtered traces (Figure 3A). This prompted us to confirm the presence of slow-γ oscillations, as well as their coordination, time-locked to the occurrence of SWR. To achieve this, we computed an additional measure of γ-frequency power, the inverse of the inter-peak interval of the wide-band γ (10-80 Hz) filtered LFP, corresponding to these epochs. We noticed the presence of a peak circa the 27Hz frequency (Figure 3B, arrows), surrounded by distinct peaks close to 20Hz and ∼50Hz, confirming our previous analyses, as well as published work concerning HIPP LFP (Carr et al., 2012). We then asked whether SWRs were consistently accompanied by increased CG-HIPP LFP slow-γ coordination, now measured as the LFP phase-locking of the slow γ-LFP (filtered now at 23-30Hz), computed, for each dataset, as the circular concentration (Kappa) of the distribution of slow-γ relative phase between the two regions, on consecutive 250ms bins surrounding HIPP SWR, normalized as before (by the baseline value corresponding to the 250ms before SWR detection). We found a post-SWR increase in the CG-HIPP slow-γ phase offset Kappa (a measure of increased LFP phase alignment, Carr et al., 2012), indicating a SWR-triggered increase in CG-HIPP coordination (Figure 3C-D, $p<0.05$, two-sample Wilcoxon Signed Rank Test comparing the 250ms bin before, with the one after SWR. The color plot in C is the average of the slow γ-phase distributions across all datasets, evaluated at 10ms-sliding 250ms windows). However, we did also see increased average slow-γ-phase offset Kappa preceding the baseline considered for analyses, in agreement with the findings presented so far, indicating, once again, that SWR-elicited slow-γ synchrony changes occur in a background of enhanced synchrony characterizing quiet wakefulness.

This analysis further confirmed that the dynamic cingulate-hippocampus coordination at slow-γ frequencies is time-locked to the occurrence of HIPP SWR.

Cingulate single neurons are phase-locked to the hippocampal LFP slow-γ during HIPP SWR

γ-oscillations are ubiquitous in the awake-behaving rat. They have been related to the transfer of contextual information between distinct areas of hippocampus and cortex (Colgin et al., 2009; Jensen and Colgin, 2007; Spellman et al., 2015; Yamamoto et al., 2014), with cortico-hippocampal slow-γ coherence recently associated with sequential choices (Cabral et al., 2014), spatial-olfactory associative learning (Igarashi et al., 2014), and specifically with

the retrieval of spatial contextual information in hippocampus (Bieri et al., 2014). In order to investigate the modulation of CG neurons by the HIPP LFP γ, and how it might be related to the SWR modulation we've described initially, we computed, for each individual CG neuron, the circular concentration (Kappa) of the CG spike HIPP LFP slow-gamma phase distributions during the SWR period, and averaged Kappa across all CG neurons before and after SWR (Figure 4A, the histograms are examples of such distributions for CG and HIPP CA1 single units for comparison). As previously mentioned, during quiet wakefulness CG single units are already tuned to the HIPP slow-γ LFP, something that further increases during SWR events (Figure 4B). Moreover, the individual CG single-unit phase concentration analysis +/-500ms of SWR revealed that CG neurons exhibit, on average, a significant post-SWR increase in their HIPP slow-γ phase circular concentration coefficient (Figure 4C, *, $p<0.05$, 0.003, Kruskal-Wallis followed by multiple comparisons), sustained thereafter. This indicates that, besides an increased CG-HIPP coordination of LFP and MUA, at the slow-γ frequency, SWR events are accompanied by an increased modulation of cingulate single units by the hippocampal slow-γ LFP. Interestingly, it also suggests that even though spikes are slow-γ synchronized in advance of SWR (Figures 4B, 2B right panel, and 2C), and LFPs are synchronized after this point (Figure 2B left panel), it is only after SWRs that CG spikes are tuned to the HIPP LFP slow-γ rhythm. This is consistent with the following scenario: spikes from CG and HIPP neurons are slow-γ-synchronous even before HIPP rhythmic inputs depolarize the CG dendrites, at which time CG neurons become phase-locked to the HIPP slow-γ rhythm and start “reading” the HIPP-replayed message (Carr et al., 2012; Pfeiffer and Foster, 2015). If indeed γ rhythms are associated with increased CG responses to HIPP SWR, then the magnitude of HIPP γ-modulation (Kappa), and the rate-modulation by HIPP SWR, should be positively correlated. To quantify CG single neuron's modulation by SWR (Δ_{SWR}) we computed the difference between the mean firing rate before and after HIPP-SWR events, and normalized the result by the average firing rate throughout the whole behavioral session (see Supplementary Figure S2 and Methods). Next, we investigated the correlation between the degree of CG single-unit phase-locking to HIPP slow-γ LFP (Kappa), and that of their modulation by HIPP-SWR events. We did this by computing the Spearman correlation coefficient between the two measures. We found that, during the SWR event, the spike phase distribution Kappa is significantly correlated with the spike rate modulation by SWR (Figure 4D, Spearman $R=0.39$, $p<0.000001$). To investigate whether what we have is specific to slow-γ, rather than a non-specific effect of broad-band depolarization during SWR, we ran the exact same computations for the surrounding β (15-21 Hz) and fast-γ (50-80Hz) oscillations, and found no significant correlations (β $R=0.095$, $p=0.17$; fast-γ $R=0.005$, $p=0.93$). There is however, still the possibility that this correlation is trivially explained by the fact that neurons exhibiting lower mean firing rates are noisier, thus generating increased SWR and phase-modulation scores, which, by contrast with the rest of the neurons, might be responsible for the existing correlations. We thus removed the effect of the mean firing rate of each neuron by computing a partial correlation, with mean firing rate as the “third variable”. We found that after accounting for this factor the significant positive correlation between SWR and slow-γ modulation is mostly unaffected ($R=0.38$, $p<0.000001$), indicating that the correlation we've seen cannot be explained by the mean firing rate of distinct cingulate neurons. The observation that the degree of phase locking of CG neurons to HIPP slow-

gamma is significantly correlated with their rate-modulation by SWR leads us to hypothesize that the HIPP slow-γ rhythm synchronizes CG with HIPP neural populations during SWR, and that the two phenomena are functionally associated (Carr et al., 2012).

Discussion

Cingulate cortex is believed to play a major role in planning and controlling behavior, and to progressively consolidate a map relating actions with consequences, and with surrounding context (Cowen et al., 2012; Einarsson and Nader, 2012; Foster et al., 1980; Frankland et al., 2004; Goshen et al., 2011; Hillman and Bilkey, 2010; Ito et al., 2003; Kennerley and Wallis, 2009; Maviel et al., 2004; Sul et al., 2010; Totah et al., 2009). SWR events during wakefulness have been recently linked to these mental functions, as they replay extended episodes of previous behavior, and possibly selectively suppress irrelevant neural activity, thus channeling useful information onto cortical targets (Davidson et al., 2009; Jadhav et al., 2012; Pfeiffer and Foster, 2013; Stark et al., 2014). No studies have so far studied neocortical activity during these periods. In fact, neocortical activity during HIPP neural replay has been studied exclusively during slow-wave sleep (Ji and Wilson, 2007; Peyrache et al., 2009, 2010; Siapas and Wilson, 1998). We now report that, while animals are alert on the behavioral apparatus, pausing between trials, cingulate neurons are increasingly modulated by the HIPP slow-γ rhythm, as reported recently for hippocampal neurons involved in the replay of past events (Carr et al., 2012; Pfeiffer and Foster, 2015). Neurons in CG cortex significantly change their firing rate during hippocampal SWR (putative memory replay events) which coincides with an increase in cingulate-hippocampal coherence of both MUA spikes and LFP at slow-γ frequencies, a phenomenon recently associated with increased performance in a sequential choice task (Cabral et al., 2014). In addition to this we have found that the degree to which CG single neurons engage in the HIPP slow-γ rhythm significantly correlates with the degree of their modulation by HIPP SWR. We hypothesize that the transient slow-γ oscillation, such as reported in (Carr et al., 2012), not only supports the intra-hippocampal coordination of SWR-induced fast replay of past episodes, but might also channel this information onto cingulate neurons to inform the planning, and control, of upcoming behavior.

The findings we now report are consistent with the following model: during active running, cingulate neurons receive theta-rhythmic place-selective hippocampal input to encode individual trajectories, and control choices (Remondes and Wilson, 2013). Between trials, cingulate neurons transiently tune-in to the hippocampal slow-γ, known to support HIPP replay of past experiences (Carr et al, 2012). When a SWR event occurs, CG neurons' depolarization occurs preferentially in synchrony with slow-γ rhythmic “packets” of HIPP neuron's spikes, encoding place-sequences from past behavioral episodes (Carr et al, 2012; Pfeiffer and Foster, 2015). Now depolarizing synchronously at slow-γ frequency, CG neurons can interpret episodic information replayed in hippocampus to direct subsequent choice behavior.

Experimental Procedures

Behavior

All procedures were performed in accordance with MIT Committee on Animal Care and NIH guidelines. Nine male Long-Evans rats (3–6 months) where used in this study, from which 31 datasets where selected. In these sessions animals: performed trials on the Wagon-wheel Maze task as described previously (Remondes and Wilson, 2013), as well as on versions of a 2m linear track, had stable isolated units recorded from cingulate cortex (CG), and tetrodes had not been adjusted within at least the previous 12 hours. Briefly, in the WWM task subjects ran repeatedly on a wagon-wheel shaped maze, and were rewarded for correctly selecting one the four available arms, towards a common reward site, according to a set sequence (1-2-3-4), as previously described (Remondes and Wilson, 2013).

Electrophysiological recordings

Data analyzed included cingulate (CG), and hippocampal (HIPP) single and multi-units' action potentials (“spikes”), field potential (LFP) and *xy* position, recorded as previously described (Remondes and Wilson, 2013). Briefly, data were obtained using an implanted microdrive array of 18 independently movable tetrodes targeting exclusively anterior CG cortex (CG, 11-9 tetrodes, 0.3 – 0.8 ML, 2.0-0.5 AP, 0-3.0 DV, mm from Bregma) and HIPP CA1 (7-9 tetrodes, 0.5 -2.5 ML, -2.0 - -4.0 AP, 3.0 DV). Position was acquired at 30Hz by an array of diodes located above the electrode drive. Analysis was restricted to stopping periods on the behavioral apparatus (less than 4 cm/sec). Data analyzed for the present work were acquired from 9 rats, for a total of 224 cingulate units, distributed over 31 datasets. The criteria for selecting these datasets were defined blind to any analysis posterior to clustering and LFP/position-based SWR extraction: stable units in cingulate cortex, the presence of ripples on the behavioral track, the absence of sleep periods, defined behaviorally as periods of sustained immobility and body posture, and physiologically by the absence of slow waves. Action potentials were assigned to individual neurons by offline, manual clustering based on the spikes' amplitudes on the four channels of each tetrode, using Xclust software (M.A. Wilson). Subsequent analyses employed code written by M. Remondes, as well from the Chronux (Bokil et al., 2010) and CircStat (Philipp Berens, 2009) toolboxes, written in Matlab (MathWorks, Natick, MA).

Supplementary Material

Refer to Web version on PubMed Central for supplementary material.

Acknowledgments

This work was supported by the National Institutes of Health, Grant 5-RO1-MH061976-09, and Fundação para a Ciência e Tecnologia – Portugal, with a postdoctoral fellowship to M. Remondes.

We are indebted to all members of the Wilson Lab for fruitful discussions on the present work, and to Daniel Bendor for also revising a final version of the manuscript.

References

Battaglia FP, Benchenane K, Sirota A, Pennartz CM, Wiener SI. The hippocampus: hub of brain network communication for memory. Trends Cogn Sci. 2011; 15:310–318. [PubMed: 21696996]

Belluscio MA, Mizuseki K, Schmidt R, Kempter R, Buzsaki G. Cross-Frequency Phase-Phase Coupling between Theta and Gamma Oscillations in the Hippocampus. J Neurosci. 2012; 32:423–435. [PubMed: 22238079]

Bieri KW, Bobbitt KN, Colgin LL. Slow and Fast Gamma Rhythms Coordinate Different Spatial Coding Modes in Hippocampal Place Cells. Neuron. 2014

Bokil H, Andrews P, Kulkarni JE, Mehta S, Mitra PP. Chronux: A platform for analyzing neural signals. J Neurosci Methods. 2010; 192:146–151. [PubMed: 20637804]

Buzsaki G. Two-stage model of memory trace formation: a role for "noisy" brain states. Neuroscience. 1989; 31:551–570. [PubMed: 2687720]

Cabral HO, Vinck M, Fouquet C, Pennartz CMA, Rondi-Reig L, Battaglia FP. Oscillatory Dynamics and Place Field Maps Reflect Hippocampal Ensemble Processing of Sequence and Place Memory under NMDA Receptor Control. Neuron. 2014; 81:402–415. [PubMed: 24462101]

Carr MF, Karlsson MP, Frank LM. Transient Slow Gamma Synchrony Underlies Hippocampal Memory Replay. Neuron. 2012; 75:700–713. [PubMed: 22920260]

Cenquizca LA, Swanson LW. Spatial organization of direct hippocampal field CA1 axonal projections to the rest of the cerebral cortex. Brain Res Rev. 2007; 56:1–26. [PubMed: 17559940]

Colgin LL, Denninger T, Fyhn M, Hafting T, Bonnevie T, Jensen O, Moser MB, Moser EI. Frequency of gamma oscillations routes flow of information in the hippocampus. Nature. 2009; 462:353–357. [PubMed: 19924214]

Cowen SL, Davis GA, Nitz DA. Anterior cingulate neurons in the rat map anticipated effort and reward to their associated action sequences. J Neurophysiol. 2012; 107:2393–2407. [PubMed: 22323629]

Davidson TJ, Kloosterman F, Wilson MA. Hippocampal replay of extended experience. Neuron. 2009; 63:497–507. [PubMed: 19709631]

Ego-Stengel V, Wilson MA. Disruption of ripple-associated hippocampal activity during rest impairs spatial learning in the rat. Hippocampus. 2010; 20:1–10. [PubMed: 19816984]

Einarsson EÖ, Nader K. Involvement of the anterior cingulate cortex in formation, consolidation, and reconsolidation of recent and remote contextual fear memory. Learn Mem. 2012; 19:449–452. [PubMed: 22984282]

Foster DJ, Wilson MA. Reverse replay of behavioural sequences in hippocampal place cells during the awake state. Nature. 2006; 440:680–683. [PubMed: 16474382]

Foster K, Orona E, Lambert RW, Gabriel M. Early and late acquisition of discriminative neuronal activity during differential conditioning in rabbits: specificity within the laminae of cingulate cortex and the anteroventral thalamus. J Comp Physiol Psychol. 1980; 94:1069–1086. [PubMed: 7204698]

Frankland PW, Bontempi B, Talton LE, Kaczmarek L, Silva AJ. The involvement of the anterior cingulate cortex in remote contextual fear memory. Science (80-). 2004; 304:881–883.

Girardeau G, Benchenane K, Wiener SI, Buzsáki G, Zugaro MB. Selective suppression of hippocampal ripples impairs spatial memory. Nat Neurosci. 2009; 12:1222–1223. [PubMed: 19749750]

Goshen I, Brodsky M, Prakash R, Wallace J, Gradinaru V, Ramakrishnan C, Deisseroth K. Dynamics of retrieval strategies for remote memories. Cell. 2011; 147:678–689. [PubMed: 22019004]

Gray CM, Singer W. Stimulus-specific neuronal oscillations in orientation columns of cat visual cortex. Proc Natl Acad Sci U S A. 1989; 86:1698–1702. [PubMed: 2922407]

Hillman KL, Bilkey DK. Neurons in the rat anterior cingulate cortex dynamically encode cost-benefit in a spatial decision-making task. J Neurosci. 2010; 30:7705–7713. [PubMed: 20519545]

Igarashi KM, Lu L, Colgin LL, Moser MB, Moser EI. Coordination of entorhinal–hippocampal ensemble activity during associative learning. Nature. 2014

Ito S, Stuphorn V, Brown JW, Schall JD. Performance monitoring by the anterior cingulate cortex during saccade countermanding. Science (80-). 2003; 302:120–122.

Jadhav SP, Kemere C, German PW, Frank LM. Awake Hippocampal Sharp-Wave Ripples Support Spatial Memory. Sci. 2012; 336:1454–1458.

Jensen O, Colgin LL. Cross-frequency coupling between neuronal oscillations. Trends Cogn Sci. 2007; 11:267–269. [PubMed: 17548233]

Ji D, Wilson MA. Coordinated memory replay in the visual cortex and hippocampus during sleep. Nat Neurosci. 2007; 10:100–107. [PubMed: 17173043]

Jones BF, Witter MP. Cingulate cortex projections to the parahippocampal region and hippocampal formation in the rat. Hippocampus. 2007; 17:957–976. [PubMed: 17598159]

Jones MW, Wilson MA. Theta rhythms coordinate hippocampal-prefrontal interactions in a spatial memory task. PLoS Biol. 2005; 3:e402. [PubMed: 16279838]

Jones BF, Groenewegen HJ, Witter MP. Intrinsic connections of the cingulate cortex in the rat suggest the existence of multiple functionally segregated networks. Neuroscience. 2005; 133:193–207. [PubMed: 15893643]

Kennerley SW, Wallis JD. Encoding of reward and space during a working memory task in the orbitofrontal cortex and anterior cingulate sulcus. J Neurophysiol. 2009; 102:3352–3364. [PubMed: 19776363]

Maviel T, Durkin TP, Menzaghi F, Bontempi B. Sites of neocortical reorganization critical for remote spatial memory. Science (80-). 2004; 305:96–99.

Peyrache A, Khamassi M, Benchenane K, Wiener SI, Battaglia FP. Replay of rule-learning related neural patterns in the prefrontal cortex during sleep. Nat Neurosci. 2009; 12:919–926. [PubMed: 19483687]

Peyrache A, Benchenane K, Khamassi M, Wiener SI, Battaglia FP. Sequential Reinstatement of Neocortical Activity during Slow Oscillations Depends on Cells' Global Activity. Front Syst Neurosci. 2010; 3:18. [PubMed: 20130754]

Pezzulo G, van der Meer MAA, Lansink CS, Pennartz CMA. Internally generated sequences in learning and executing goal-directed behavior. Trends Cogn Sci. 2014

Pfeiffer BE, Foster DJ. Hippocampal place-cell sequences depict future paths to remembered goals. Nature. 2013; 497:74–79. [PubMed: 23594744]

Pfeiffer BE, Foster DJ. Autoassociative dynamics in the generation of sequences of hippocampal place cells. Sci. 2015; 349:180–183.

Philipp, Berens. CircStat: A MATLAB Toolbox for Circular Statistics. J Stat Softw. 2009; 31:1–21.

Remondes M, Schuman EM. Direct cortical input modulates plasticity and spiking in CA1 pyramidal neurons. Nature. 2002; 416:736–740. [PubMed: 11961555]

Remondes M, Wilson MA. Cingulate-hippocampus coherence and trajectory coding in a sequential choice task. Neuron. 2013; 80:1277–1289. [PubMed: 24239123]

Siapas AG, Wilson MA. Coordinated interactions between hippocampal ripples and cortical spindles during slow-wave sleep. Neuron. 1998; 21:1123–1128. [PubMed: 9856467]

Siapas AG, Lubenov EV, Wilson MA. Prefrontal phase locking to hippocampal theta oscillations. Neuron. 2005; 46:141–151. [PubMed: 15820700]

Spellman T, Rigotti M, Ahmari SE, Fusi S, Gogos JA, Gordon JA. Hippocampal-prefrontal input supports spatial encoding in working memory. Nature. 2015 advance on.

Squire, LL.; Cohen, NJ.; Nadel, NJ. The medial temporal region and memory consolidation: A new hypothesis. In: Weingartner, H.; Parker, E., editors. Memory Consolidation. Hillsdale, NJ: Erlbaum, L.; 1984. p. 185-210.

Stark E, Roux L, Eichler R, Senzai Y, Royer S, Buzsáki G. Pyramidal Cell-Interneuron Interactions Underlie Hippocampal Ripple Oscillations. Neuron. 2014; 83:467–480. [PubMed: 25033186]

Sul JH, Kim H, Huh N, Lee D, Jung MW. Distinct roles of rodent orbitofrontal and medial prefrontal cortex in decision making. Neuron. 2010; 66:449–460. [PubMed: 20471357]

Totah NK, Kim YB, Homayoun H, Moghaddam B. Anterior cingulate neurons represent errors and preparatory attention within the same behavioral sequence. J Neurosci. 2009; 29:6418–6426. [PubMed: 19458213]

Wilson MA, Varela C, Remondes M. Phase organization of network computations. Curr Opin Neurobiol. 2015; 31C:250–253. [PubMed: 25679370]

Yamamoto J, Suh J, Takeuchi D, Tonegawa S. Successful execution of working memory linked to synchronized high-frequency gamma oscillations. Cell. 2014; 157:845–857. [PubMed: 24768692]

Young CK, McNaughton N. Coupling of theta oscillations between anterior and posterior midline cortex and with the hippocampus in freely behaving rats. Cereb Cortex. 2009a; 19:24–40. [PubMed: 18453538]

Young CK, McNaughton N. Coupling of theta oscillations between anterior and posterior midline cortex and with the hippocampus in freely behaving rats. Cereb Cortex. 2009b; 19:24–40. [PubMed: 18453538]

Zhang K, Ginzburg I, McNaughton BL, Sejnowski TJ. Interpreting neuronal population activity by reconstruction: unified framework with application to hippocampal place cells. J Neurophysiol. 1998; 79:1017–1044. [PubMed: 9463459]

Highlights

Neurons in cingulate cortex (CG) respond to hippocampal SWR, in alert rats.

Cingulate and hippocampal neural activity exhibit a SWR-triggered increase in slow-γ coordination.

SWR modulation of CG single-units correlates with their phase-locking to the hippocampal slow-γ.

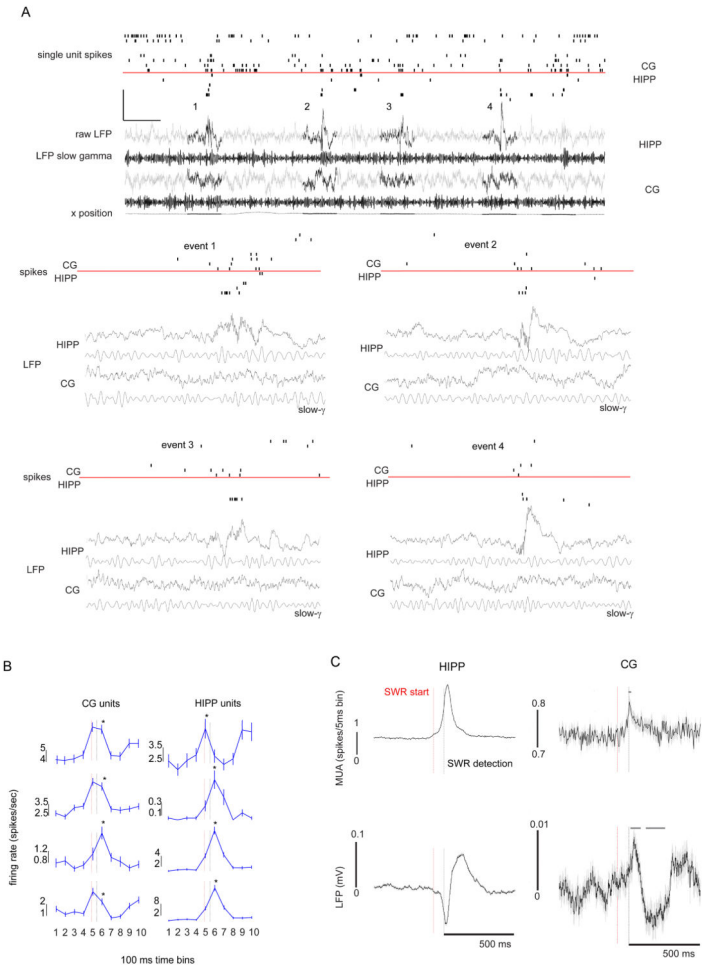

Figure 1. Cingulate cortical neurons increase their firing during hippocampal SWR

(A) Data corresponding to ∼10 seconds of activity from 8 CG and 7 HIPP single neurons (spikes from distinct anatomical regions separated by a red horizontal line), followed by raw (gray, darkened are 1 sec periods containing SWR events) and γ-filtered (black) LFP voltage, and the x-coordinate of the rat's position on the maze (xposition, also darkened on the 1 sec SWR periods). Note the presence of SWR during periods of reduced mobility ("quiet alertness"), the first four events numbered 1-4, the firing of subsets of CG and HIPP units aligned with hippocampal SWR, and the transient increases in hippocampal LFP γ amplitude. Calibration bars represent 1sec, 1(raw) and 0.5 (filtered) mV, and 150 cm for x-position. The 4 numbered events are depicted (zoomed-in in time only, 1 sec duration per event) below the main panel. (B) CG neurons (40/224, 18%, of all recorded neurons) and HIPP neurons (211/281, 75%), modulate their firing rate relative to SWR onset (*, $p<0.05$, Kruskal-Wallis followed by *post-hoc* comparisons), shown are the firing rates from four of the neurons in panel A, for each anatomical region. All plots depict the mean+/-SEM spikes/sec surrounding the ripple trigger time (black vertical line, the red line corresponds to the average-estimated SWR start, see below). Vertical calibration bars are spikes/second. (C) Summary plot of the mean CG and HIPP putative excitatory spikes and LFP, across all SWR events, showing a significant SWR modulation of CG activity (grey bar, $p<0.000001$, Kruskal-Wallis followed by *post-hoc* comparisons). On all plots the black vertical line

corresponds to the time the SWR extraction algorithm detected a SWR event (MUA/LFP ripple power 3SD above mean), the red vertical line corresponds to the point at which there was, on average, a significant increase in hippocampal MUA or LFP activity, which we estimated as, on average, the SWR starting point (80ms before the detection time). The horizontal grey bars on the cingulate (CG) activity plots mark the points in which neural activity significantly changed. In both MUA and LFP this occurs, on average, after the SWR detection point (vertical grey line). Calibration bars for each region's neural activity rates (spikes/5msec, or mV). Error bars are mean+/-SEM.

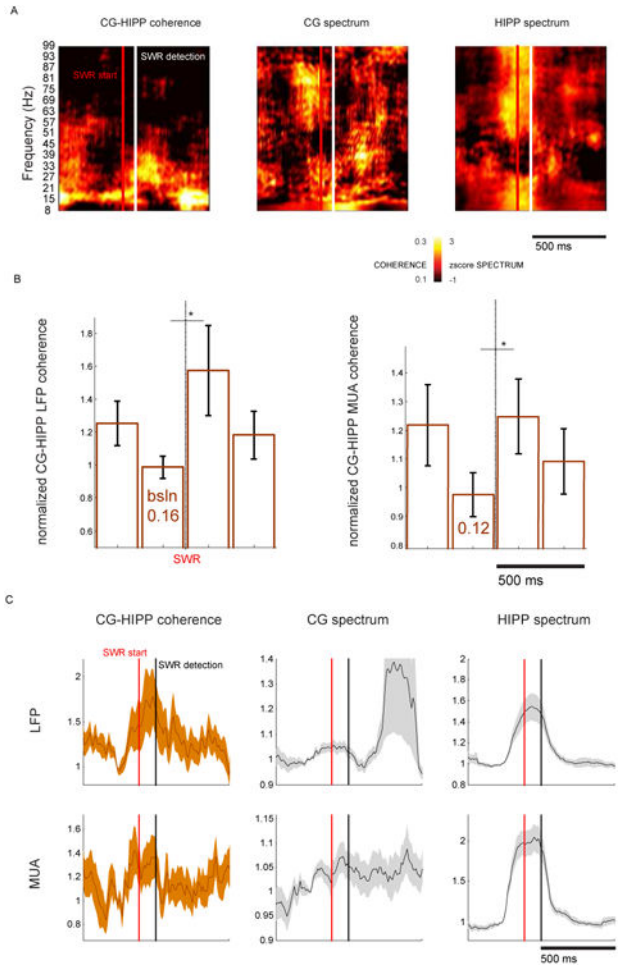

Figure 2. Increased coherence between cingulate cortex and hippocampus LFP, specific to slow-γ rhythms

(A) Example coherogram between CG and HIPP raw LFP (Methods), followed by CG and HIPP z-scored spectrograms computed on the same data. Note the presence of CG-HIPP coherence and power within the β–γ range, present during SWR (white bar: SWR trigger). As before, we added a vertical red bar to mark the estimated beginning of the SWR event. (B) Analysis of LFP (left) and MUA (right) coherence on non-overlapping 250 ms time intervals, +/- 500 ms around SWR onset, at 27Hz frequency (representative of the frequency range in which we found a SWR-related significant difference in LFP and MUA coherence,*, $p<0.05$, two-sample Wilcoxon Signed Rank Test). Numbers inside the bars are the pre-SWR baseline. Error bars are mean+/-SEM. (C) Time-resolved analysis of slow-γ coherence and power +/-500ms of SWR. Note the peak in MUA coherence before SWR estimated starting point (vertical red line in all plots). A peak in the CG slow-γ power ∼300 post-SWR can also be seen, accompanied by considerably increased error. This is due to 4 datasets in which such increase is ∼6× the baseline. While this is matter for future inquiry, it is not something we find consistently across the datasets analyzed here, and as such we do not make any further claims or comments.

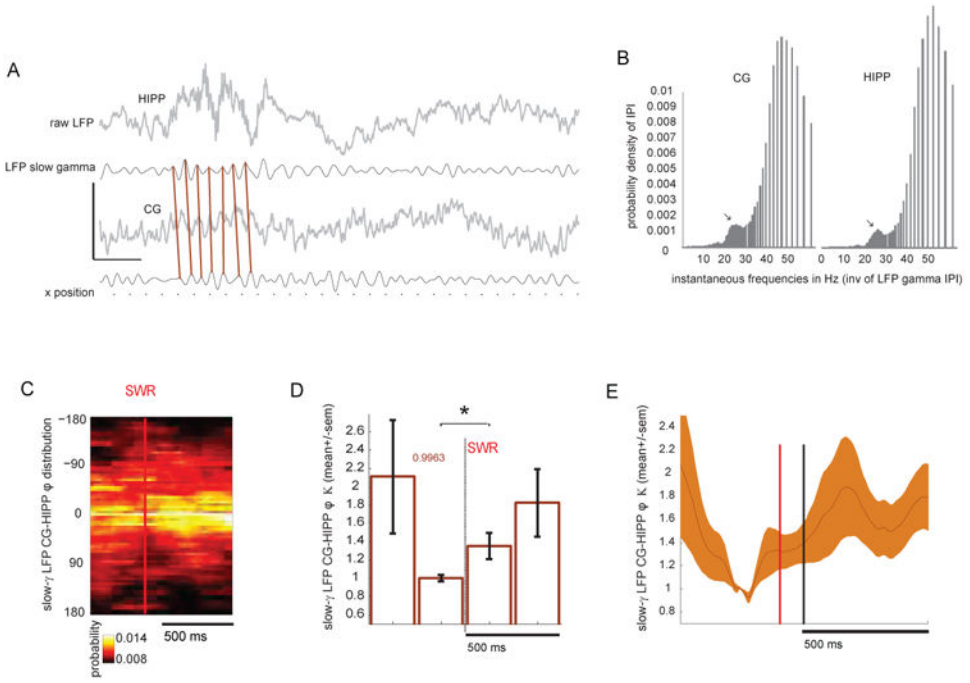

Figure 3. Phase-locking of cingulate and hippocampal slow-γ LFP during HIPP SWR

(A) Raw and γ-filtered hippocampal and cingulate LFP encompassing a SWR event. Note the peak-to-peak correspondence between LFP traces, highlighted by the diagonal bars. Calibration bars represent 1sec, 1(raw) and 0.5 (filtered) mV, and 150 cm for x-position. Calibration bars represent 250ms and 1(raw) and 0.5 (filtered) mV (B) Instantaneous CG and HIPP phase, computed from the distribution of the inverse inter-peak interval of the γ-filtered LFP, during SWR. Note the presence of a distinct peak (arrows) at slow-γ frequency (~27Hz) on both CG and HIPP. Additional peaks are present just before 20Hz and at 50Hz. (C) Color plot depicts the dataset-averaged distribution of CG-HIPP slow-γ phase-offsets +/-500ms of SWR events. Note the increase in the concentration of phase-offset distributions post-SWR detection. (D) Circular concentration (Kappa) of CG and HIPP slow-γ phase offsets, averaged across all datasets on non-overlapping 250ms time bins exhibits a significant increase in the 250ms post-SWR, compared to the pre-SWR baseline (*, $p<0.05$, two-sample Wilcoxon Signed Rank Test). Colored number “0.9963” is the pre-SWR mean baseline of the offset KAPPA. (E) Same data but the plot includes all the overlapping 250ms bins (sliding by 10ms). Error bars are mean+/-SEM.

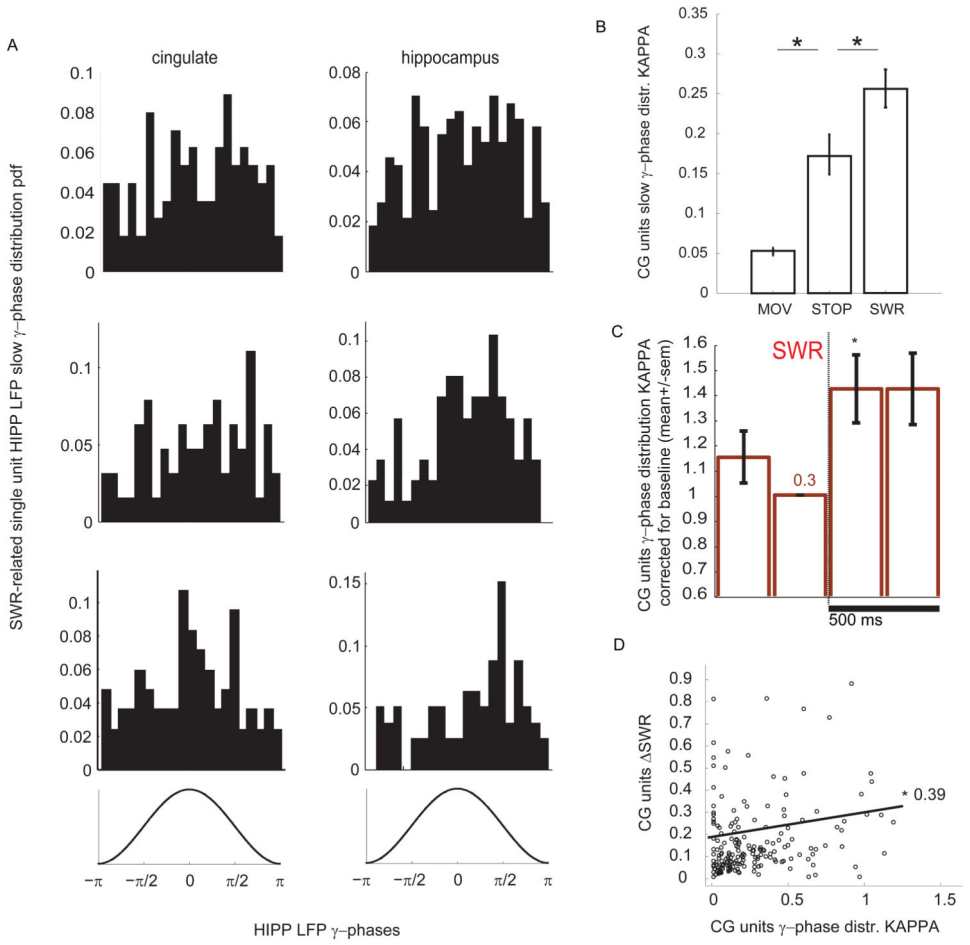

Figure 4. Phase-locking of cingulate cortical neurons to the hippocampal slow-γ rhythm is correlated with their modulation by SWR

(A) Examples of cingulate (left col), as well as hippocampal (right col) single units' spikes slow-γ phases histograms, showing single-neurons phase-locked to the HIPP slow-γ LFP for the +/- 500ms SWR period. Consecutive slow-γ phases are depicted at the bottom of the panel for guidance. (B) Average single-unit slow-γ distribution Kappa, across all recorded CG single units, showing an increase with changing behavioral state, from movement (MOV) to motionless (STOP) and SWR epochs (*, $p<0.05$, Kruskal-Wallis followed by post-hoc comparisons). (C) Phase locking (Kappa) of all CG single-units to the HIPP slow-γ LFP increases significantly post-SWR (*, $p<0.05$, Kruskal-Wallis followed by *post-hoc* comparisons). Number “0.3” inside the bar is the pre-SWR mean baseline single-unit slow-γ KAPPA. (D) Significant correlation between γ-phase distribution Kappa and SWR modulation (Methods), computed during HIPP SWR (see Methods), Spearman R=0.39, $p<0.000001$. Error bars are mean+/-SEM.